

Electronic Supplementary Information (ESI) for Journal of Materials Chemistry A
This journal is © The Royal Society of Chemistry 2020

Facile modulation of different vacancies in ZnS nanoplates for efficient solar fuel production

Pan Li,^{a,b} Lingju Guo,^a Shuangming Chen,^c Gan Luo,^b Shuang Zhu,^{a,d} Yanjie Wang,^a Li Song *^c and Tao He*^{a,d}

^a CAS Key Laboratory of Nanosystem and Hierarchical Fabrication, CAS Center for Excellence in Nanoscience, National Center for Nanoscience and Technology, Beijing 100190, China. E-mail: het@nanoctr.cn

^b Henan Engineering Center of New Energy Battery Materials, Henan D&A Engineering Center of Advanced Battery Materials, School of Chemistry and Chemical Engineering, Shangqiu Normal University, Shangqiu, Henan 476000, China

^c National Synchrotron Radiation Laboratory, CAS Center for Excellence in Nanoscience, University of Science and Technology of China, Hefei, Anhui 230029, China. E-mail: song2012@ustc.edu.cn

^d University of Chinese Academy of Sciences, Beijing 100049, China.

Fig. S1. TGA and DTG results of ZnS(en)_{0.5} precursor measured in (a) Ar and (b) air atmosphere, respectively.

Fig. S2. (a) Raman and (b) FT-IR spectra of ZnS(en)_{0.5}, ZnS-Ar and ZnS-Air samples, respectively.

Fig. S3. Solar fuel production over ZnS-Ar and ZnS-Air catalysts, respectively.

Fig. S4. XRD patterns of the ZnS samples before and after photoreduction experiments.

Fig. S5. High resolution XPS spectra of (a) Zn 2p and (b) S 2p of the ZnS samples after photoreduction experiments.

Fig. S6. SEM images of (a) ZnS-Ar and (b) ZnS-air samples after photoreduction experiments.

Fig. S7. EIS Nyquist plot of the samples before and after photoreduction experiments and the zoom-in spectra.

Fig. S8. Solar fuel production over ZnS-Ar sample for 8 h.

Fig. S9. EDX mapping of the ZnS samples prepared in Ar and air, respectively.

Fig. S10. XRD pattern of commercial ZnS used as reference sample, indicating it is Blende structure.

Fig. S11. SEM images of commercial ZnS used as reference sample.

Fig. S12. Distribution of pore size for ZnS-Ar (3.5 ± 1.0 nm) and ZnS-Air ($\sim 2.0\text{-}15.0$ nm) samples.

Fig. S13. PL spectra of the ZnS samples synthesized in Ar and air, respectively.

Fig. S14. Typical isotherms of (a) CO₂ adsorption and (b) N₂ adsorption-desorption for ZnS-Ar and ZnS-Air samples.

Fig. S15. Adsorption configurations of (a) CO, (b) H₂O and (c) H₂ on the clean surface, V_s defects and V_{Zn}-V_s-V_{Zn} defects of ZnS, respectively.

Fig. S16. In-situ DRIFTS for CO₂ interactions with ZnS catalysts in the dark and under irradiation.

Fig. S17. In-situ DRIFTS for the interactions of intermediates formed during CO₂ photoreduction with ZnS catalysts in the dark and under irradiation.

Fig. S18. In-situ DRIFTS for H₂O interactions with ZnS catalysts in the dark and under irradiation.

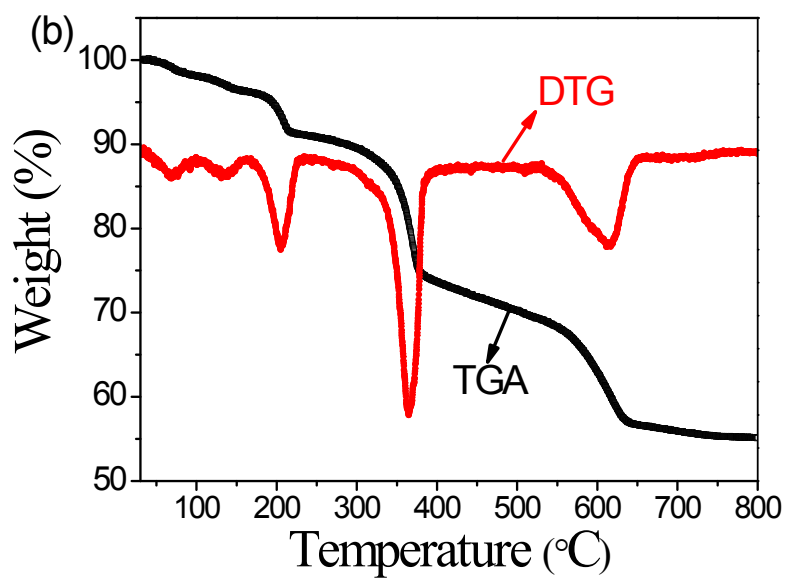
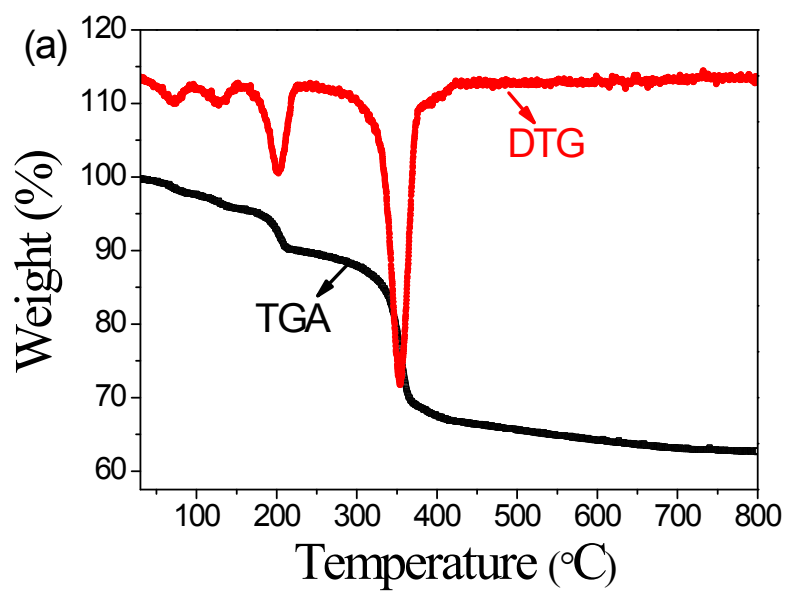


Fig. S1. TGA and DTG results of $\text{ZnS}(\text{en})_{0.5}$ precursor measured in (a) Ar and (b) air atmosphere, respectively.

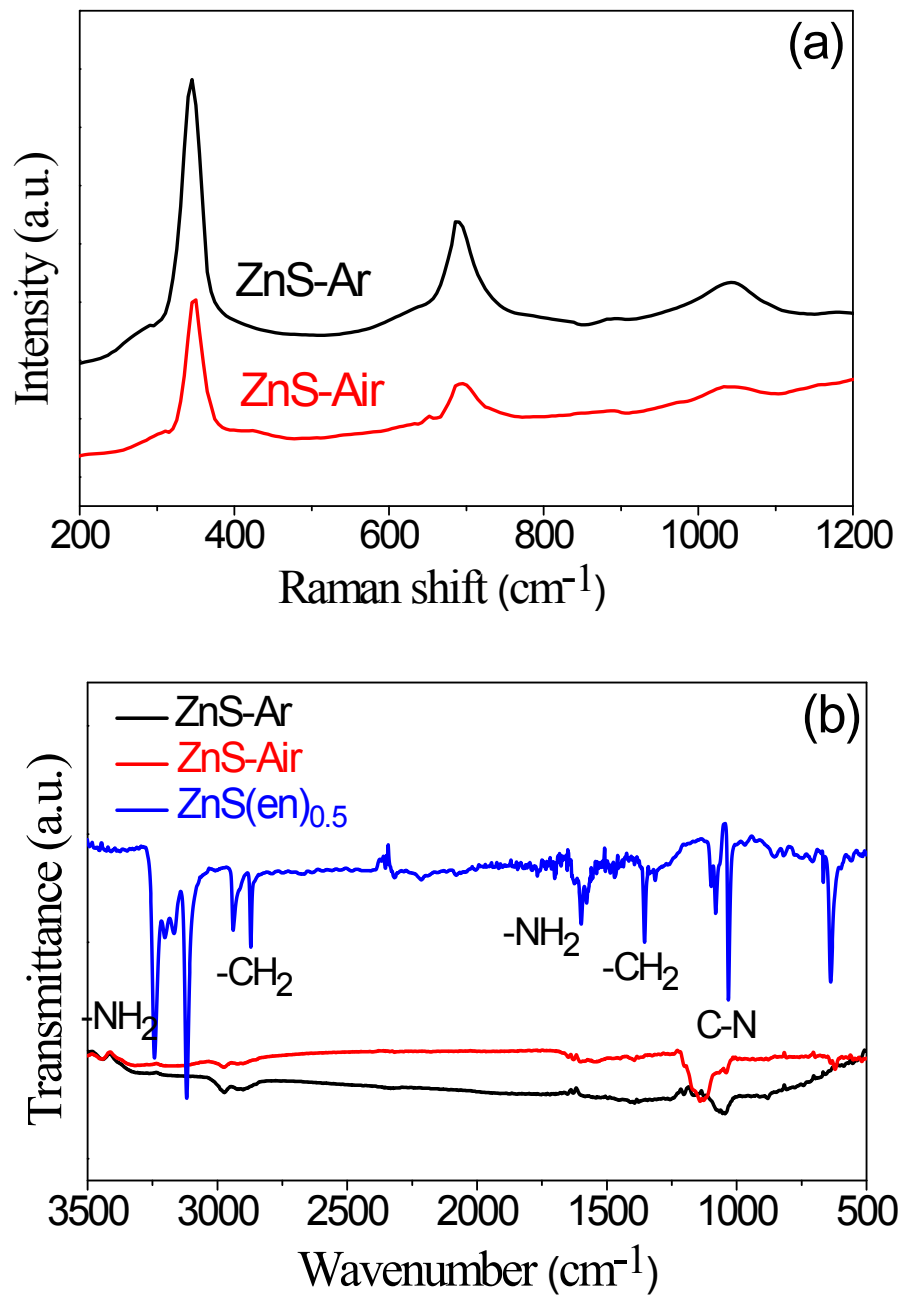


Fig. S2. (a) Raman and (b) FT-IR spectra of $\text{ZnS}(\text{en})_{0.5}$, ZnS-Ar and ZnS-Air samples, respectively.

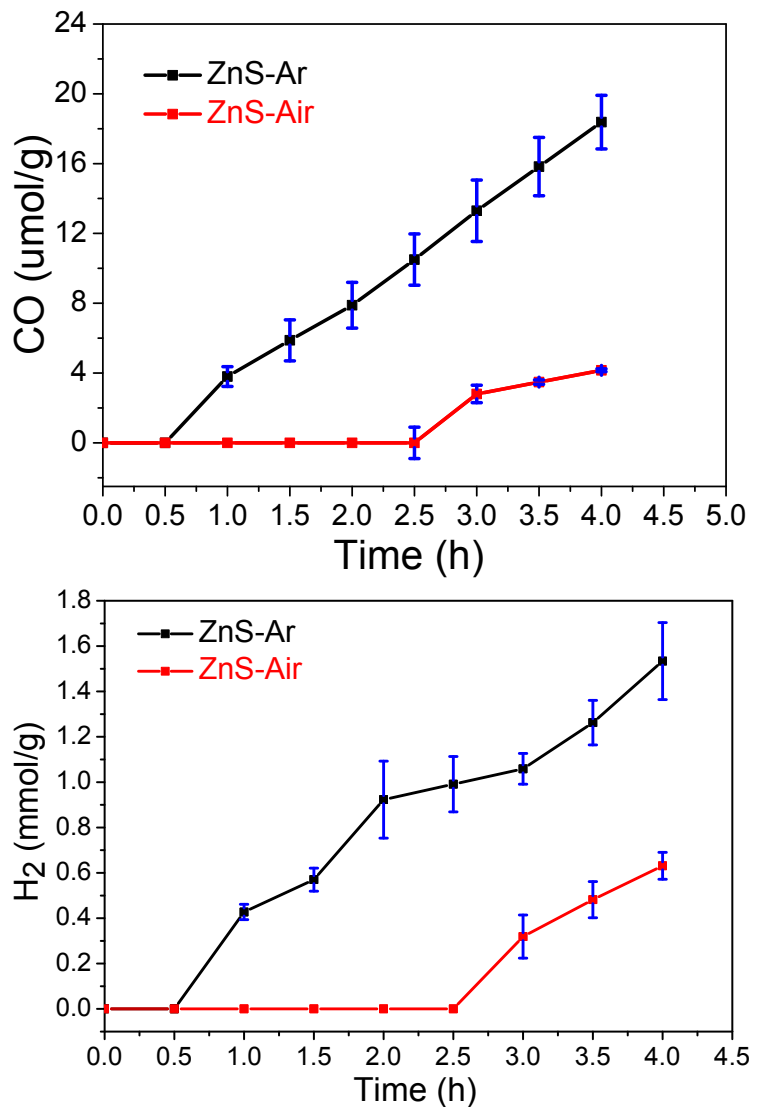


Fig. S3. Solar fuel production over ZnS-Ar and ZnS-Air catalysts, respectively.

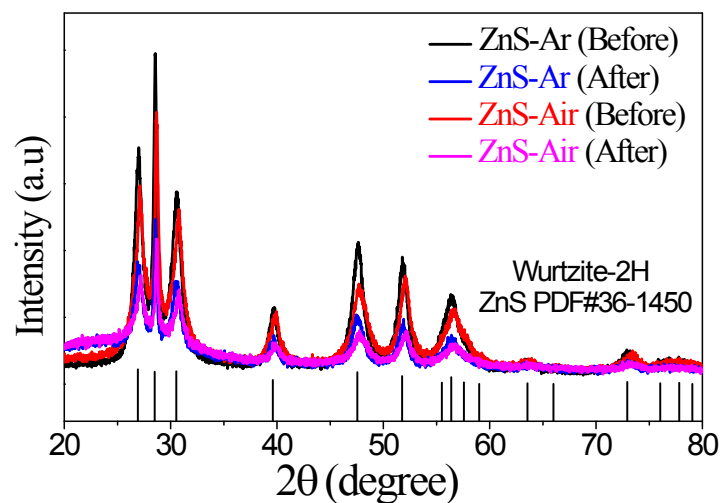


Fig. S4. XRD patterns of the ZnS samples before and after photoreduction experiments.

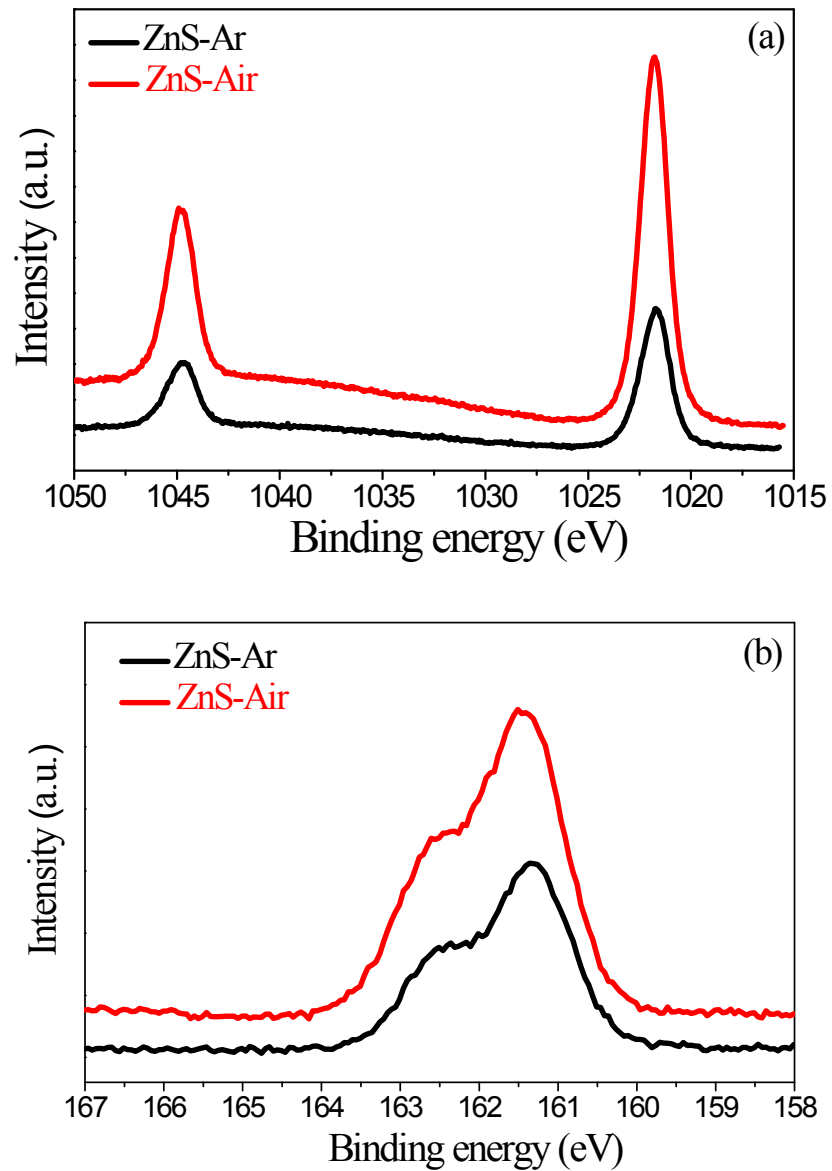


Fig. S5. High resolution XPS spectra of (a) Zn 2p and (b) S 2p of the ZnS samples after photoreduction experiments.

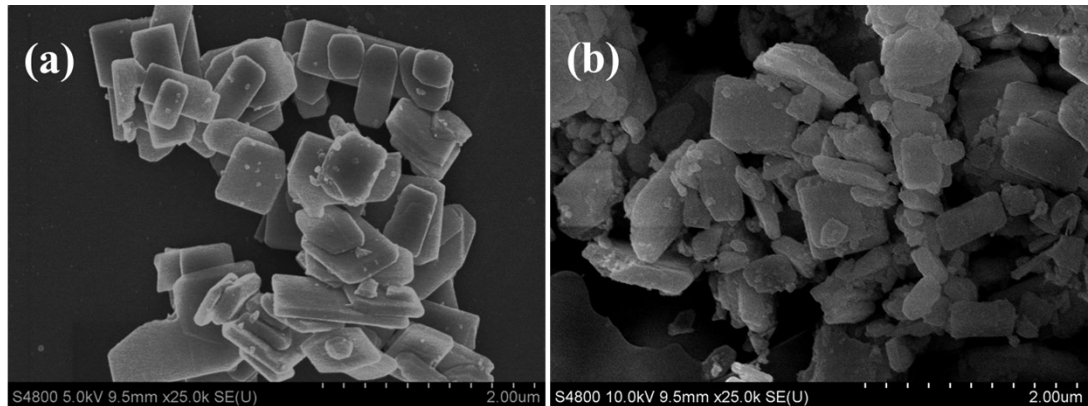


Fig. S6. SEM images of (a) ZnS-Ar and (b) ZnS-Air samples after photoreduction experiments.

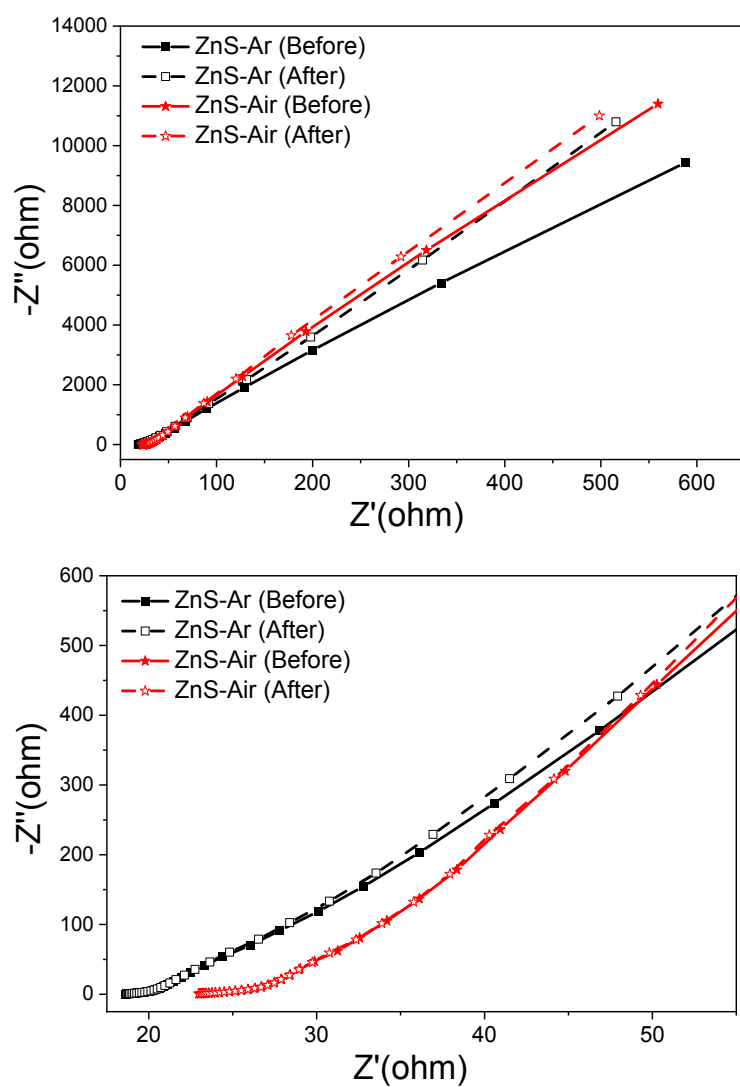


Fig. S7. (Top) EIS Nyquist plot of the samples before and after photoreduction experiments and (Bottom) the zoom-in spectra.

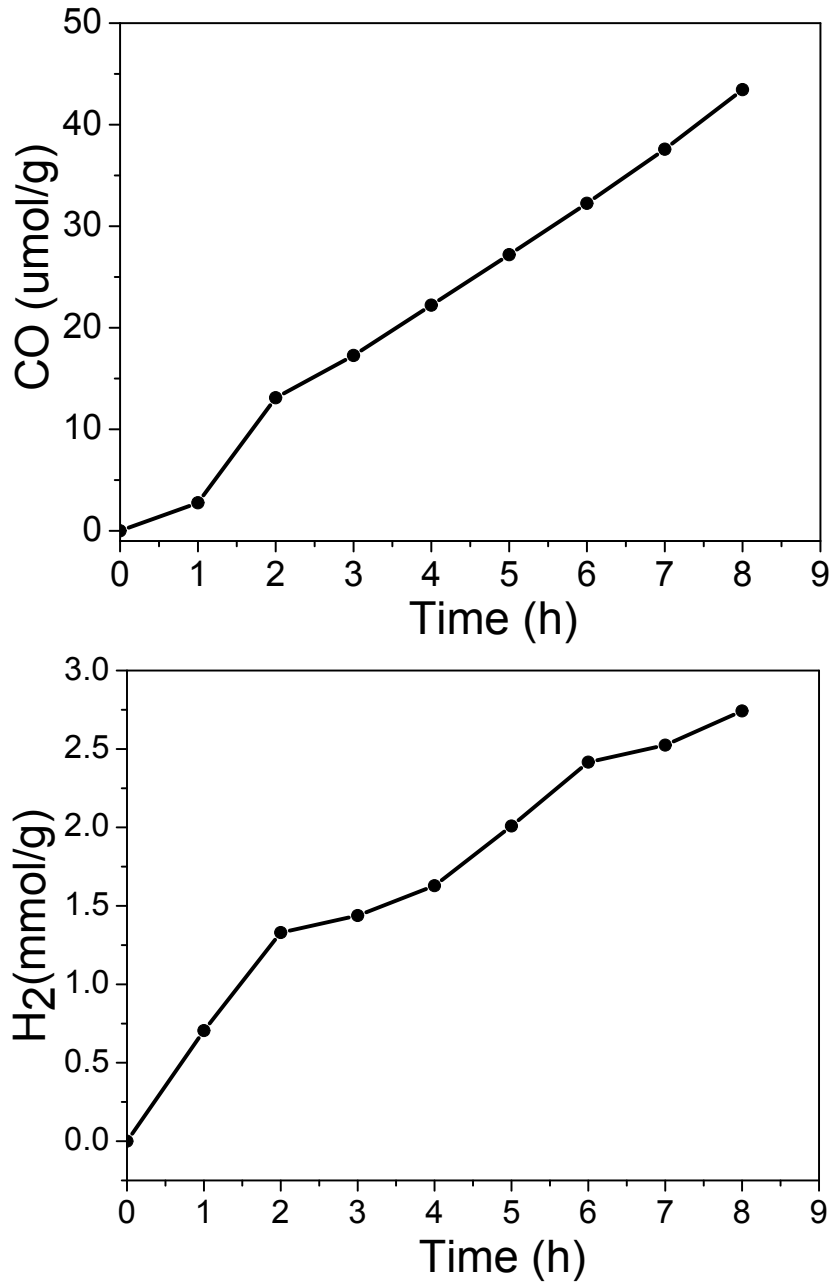


Fig. S8. Solar fuel production over ZnS-Ar sample for 8 h.

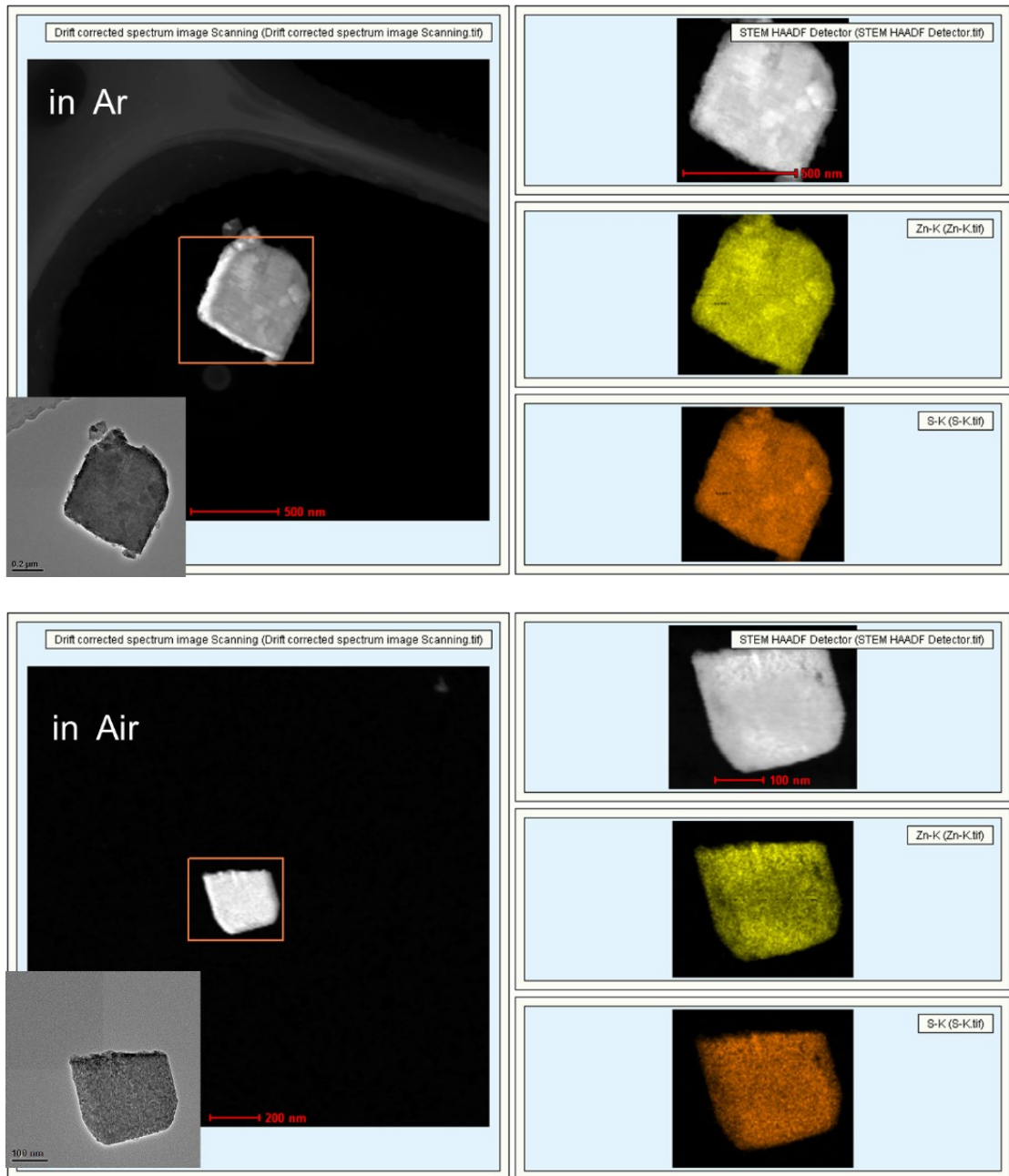


Fig. S9. EDX mapping of the ZnS samples prepared in Ar and air, respectively.

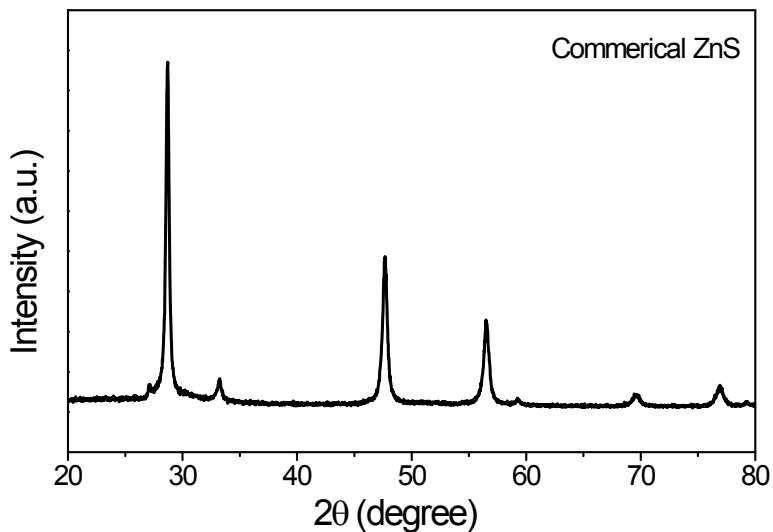


Fig. S10. XRD pattern of commercial ZnS used as reference sample, indicating it is Blende structure.

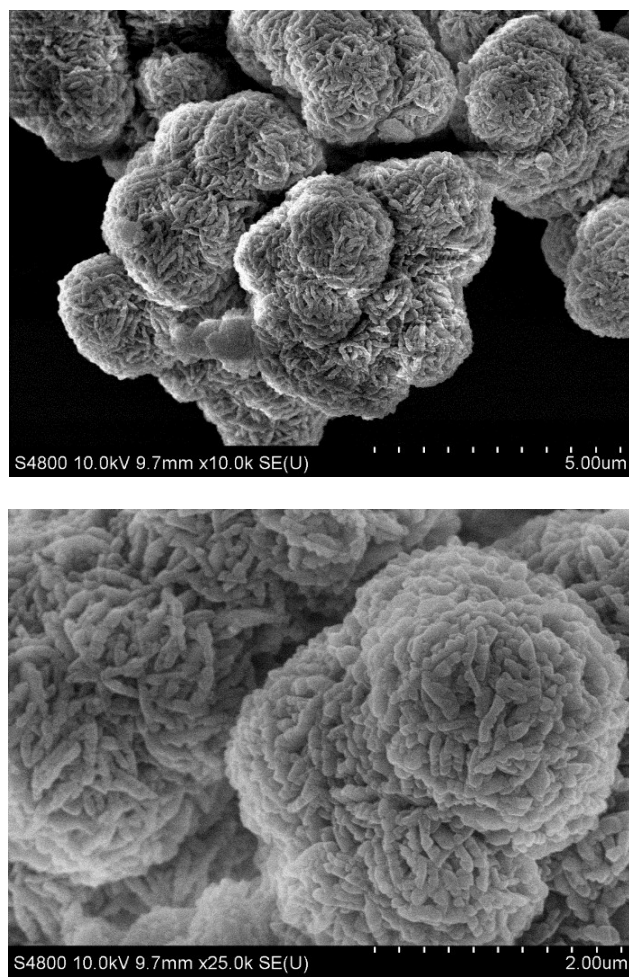


Fig. S11. SEM images of commercial ZnS used as reference sample.

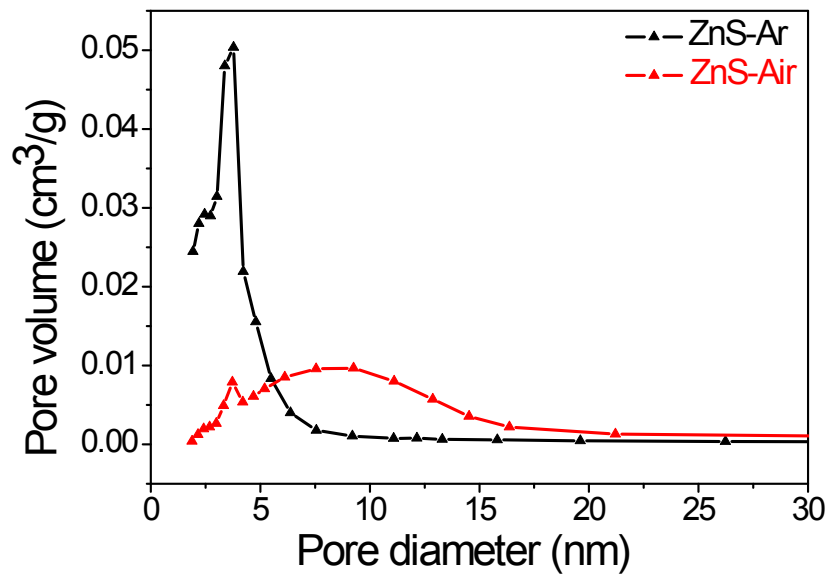


Fig. S12. Distribution of pore size for ZnS-Ar (3.5 ± 1.0 nm) and ZnS-Air ($\sim 2.0\text{-}15.0$ nm) samples.

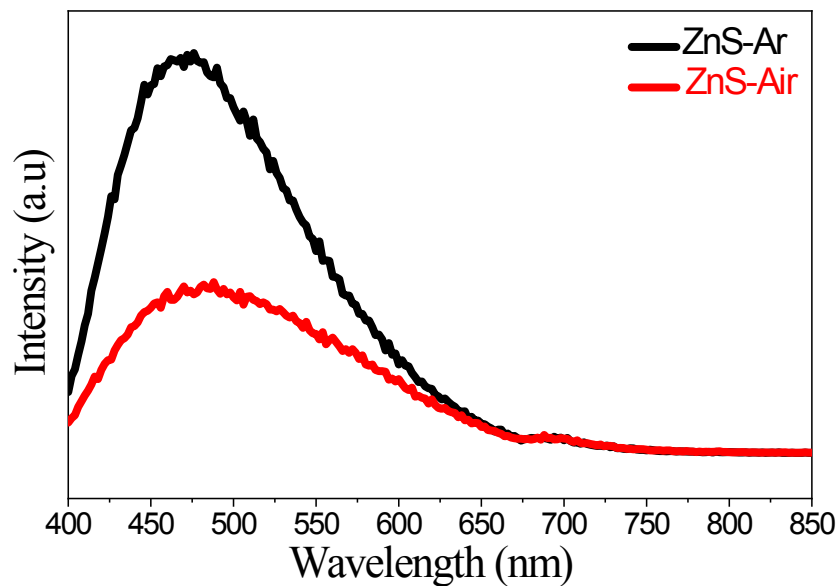


Fig. S13. PL spectra of the ZnS samples synthesized in Ar and air, respectively.

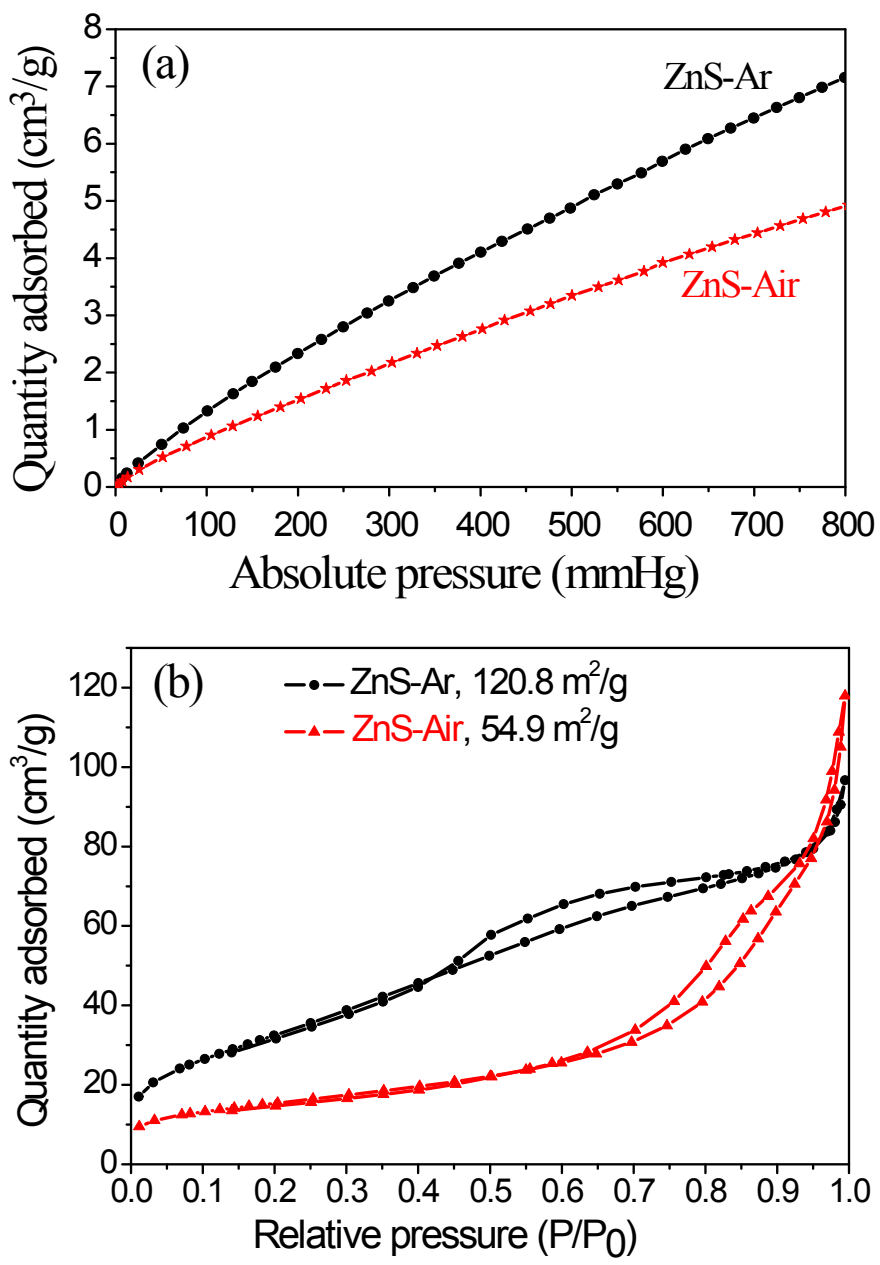


Fig. S14. Typical isotherms of (a) CO_2 adsorption and (b) N_2 adsorption-desorption for ZnS-Ar and ZnS-Air samples.

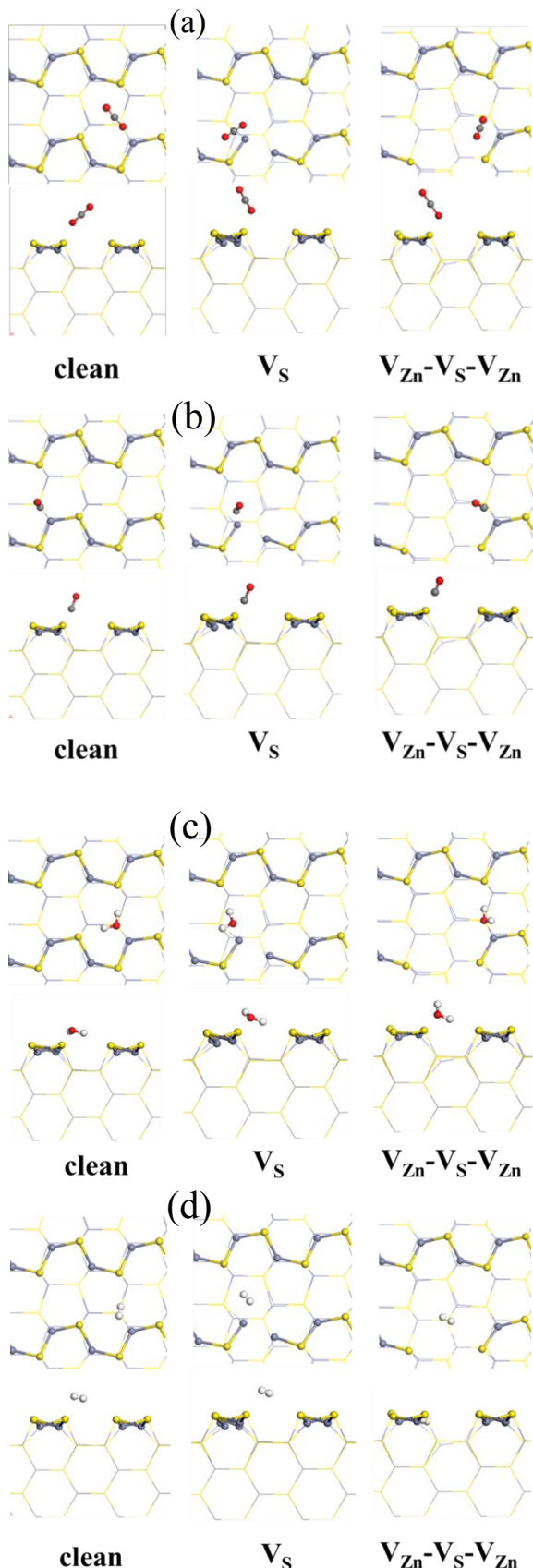


Fig. S15. Adsorption configurations of (a) CO_2 , (b) CO , (c) H_2O , and (d) H_2 on the clean surface, V_s defects, and $V_{\text{Zn}}-\text{V}_s-\text{V}_{\text{Zn}}$ defects of ZnS , respectively.

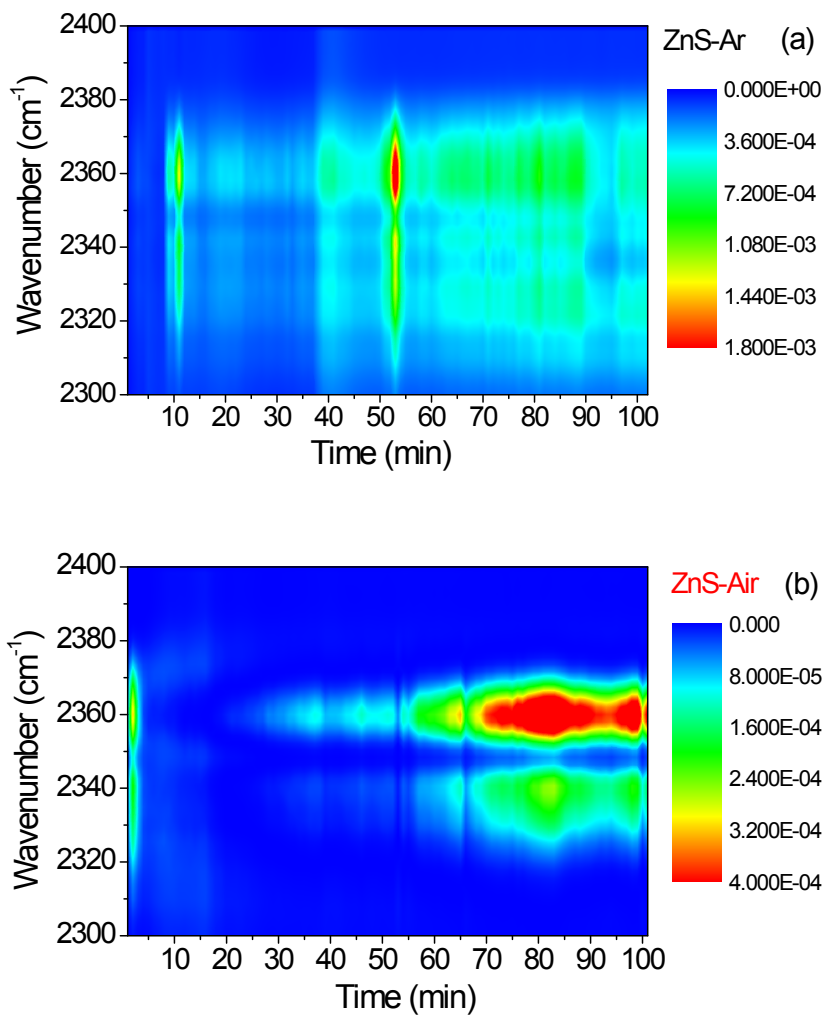


Fig. S16. In-situ DRIFTS for CO₂ interactions with ZnS catalysts in the dark and under irradiation.

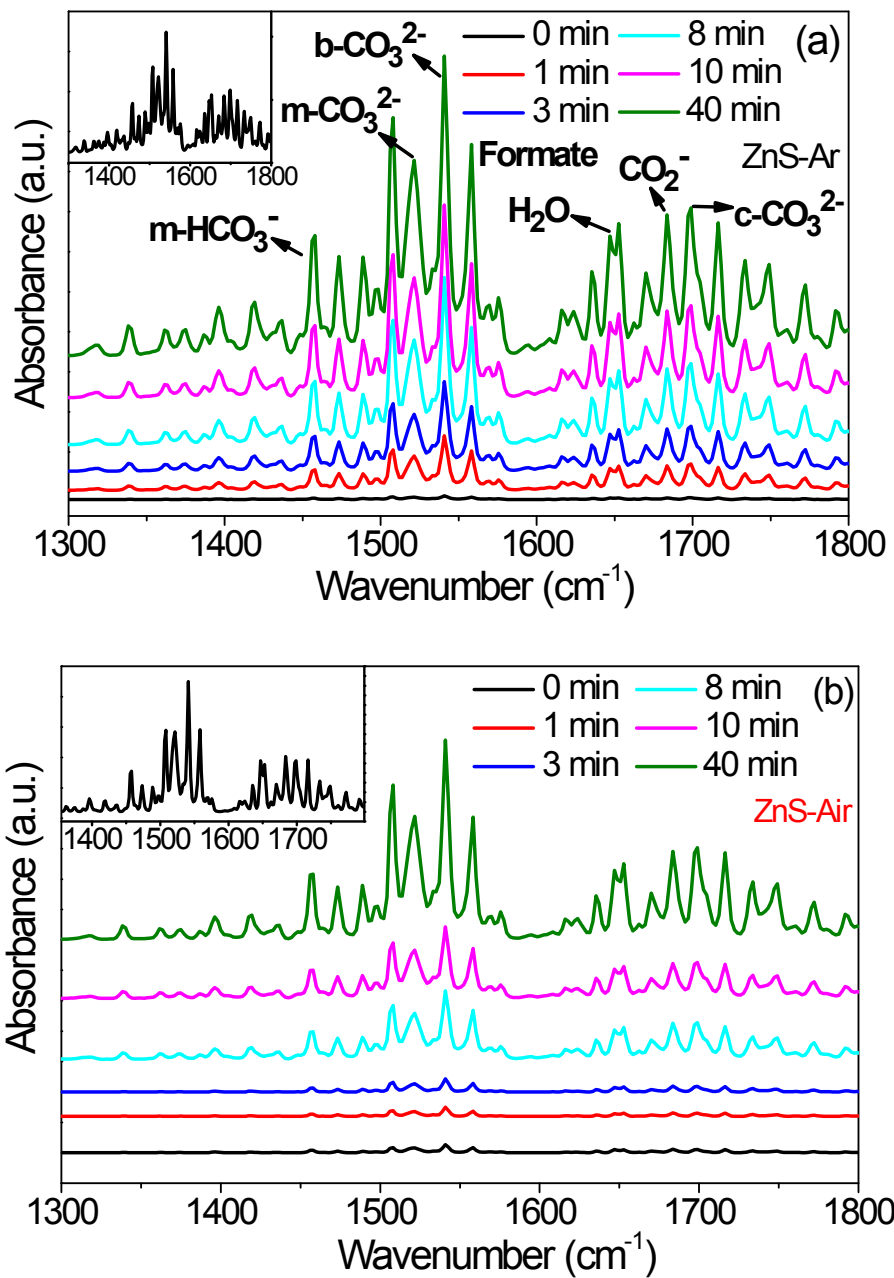


Fig. S17. In-situ DRIFTS for the interactions of intermediates formed during CO_2 photoreduction with ZnS catalysts in the dark and under irradiation.

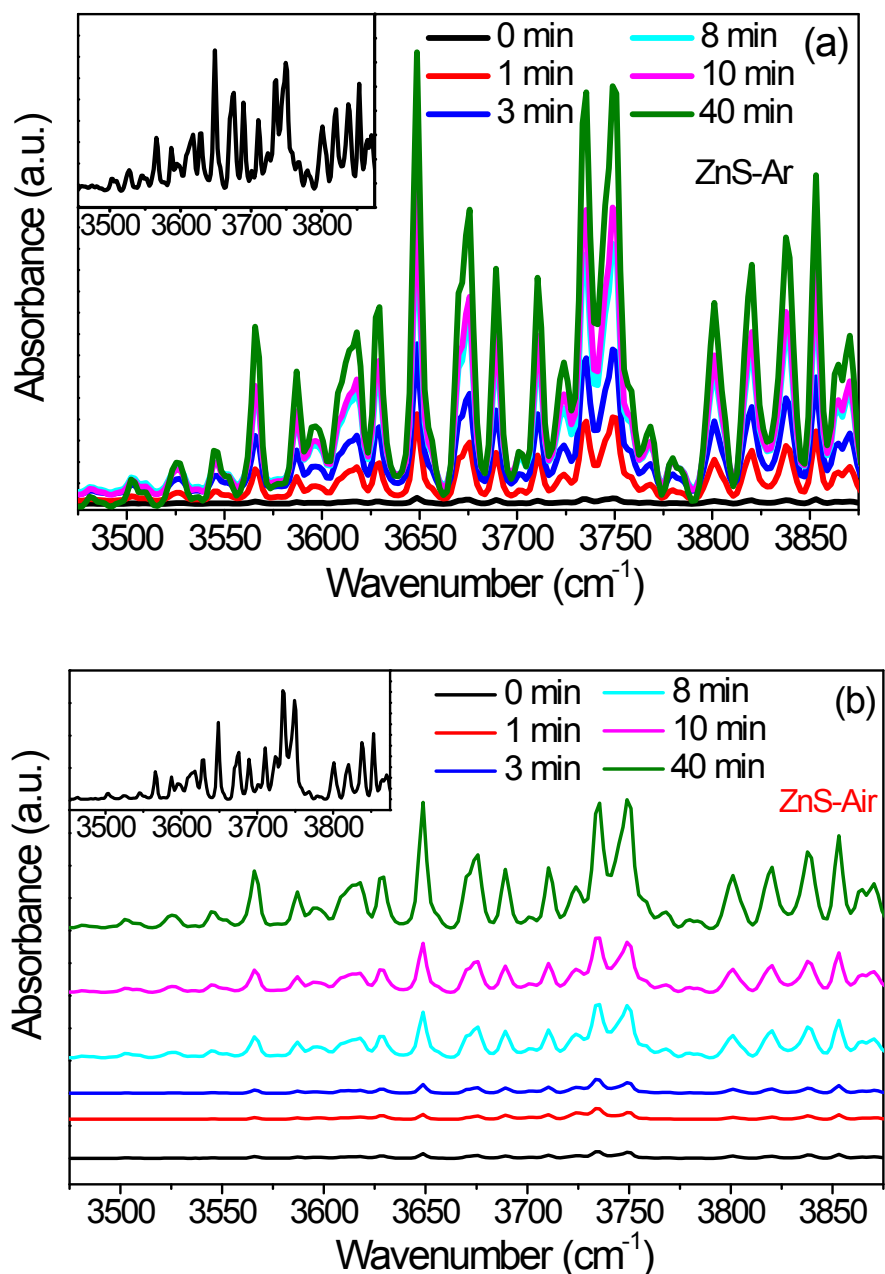


Fig. S18. In-situ DRIFTS for H_2O interactions with ZnS catalysts in the dark and under irradiation.